International Journal of Nanomedicine

Dovepress
open access to scientific and medical research

Open Access Full Text Article

ORIGINAL RESEARCH

Micropatterned nanolayers immobilized with nerve growth factor for neurite formation of PC12 cells

This article was published in the following Dove Press journal:
International Journal of Nanomedicine

Seong Min Kim[1,2]
Masashi Ueki[1]
Xueli Ren[3]
Jun Akimoto[1]
Yasuyuki Sakai[2]
Yoshihiro Ito[1,3]

[1]Nano Medical Engineering Laboratory, RIKEN Cluster for Pioneering Research, Wako, Saitama 351-0198, Japan; [2]Department of Bioengineering, School of Engineering, The University of Tokyo, Tokyo 113-8656, Japan; [3]Emergent Bioengineering Materials Research Team, RIKEN Center for Emergent Matter Science, Wako, Saitama 351-0198, Japan

Background: Nerve regeneration is important for the treatment of degenerative diseases and neurons injured by accidents. Nerve growth factor (NGF) has been previously conjugated to materials for promotion of neurogenesis.

Materials and methods: Photoreactive gelatin was prepared by chemical coupling of gelatin with azidobenzoic acid (P-gel), and then NGF was immobilized on substrates in the presence or absence of micropatterned photomasks. UV irradiation induced crosslinking reactions of P-gel with itself, NGF, and the plate for immobilization.

Results: By adjustment of the P-gel concentration, the nanometer-order height of micropatterns was controlled. NGF was quantitatively immobilized with increasing amounts of P-gel. Immobilized NGF induced neurite outgrowth of PC12 cells, a cell line derived from a pheochromocytoma of the rat adrenal medulla, at the same level as soluble NGF. The immobilized NGF showed higher thermal stability than the soluble NGF and was repeatedly used without loss of biological activity. The 3D structure (height of the formed micropattern) regulated the behavior of neurite guidance. As a result, the orientation of neurites was regulated by the stripe pattern width.

Conclusion: The micropattern-immobilized NGF nanolayer biochemically and topologically regulated neurite formation.

Keywords: nerve growth factor, photoreactive gelatin, micropatterned immobilization, PC12 cell, neurite outgrowth

Introduction

Neural regeneration is a crucial issue for the treatment of neurodegenerative diseases and injured neurons.[1] Neural tissue engineering is rapidly becoming a growing field for the discovery of new methods to regenerate the nervous system.[2–6] To regenerate neural systems, immobilization of nerve growth factor (NGF) has been considered to be useful for material development, because it is one of the neurotrophic factors that plays an important role in neuron survival and neurite outgrowth.

Immobilization of NGF has been performed using various kinds of materials such as gelatin,[7] poly(2-hydroxyethylmethacrylate) gel,[8] photoreactive chitosan,[9] and allylamine-grafted glass.[10] Because the growth cone is guided according to the concentration gradient of NGF,[11] gradient immobilization has been performed.[12,13] By immobilization of NGF and semaphorin A, regulated guidance of axonal growth has been achieved.[14–16]

To enhance the activity of immobilized NGF, co-immobilization with the extracellular matrix protein laminin has been employed.[17] Because electrical signals are also one of the factors that enhance such activity,[18] NGF has been immobilized on

Correspondence: Yoshihiro Ito
Nano Medical Engineering Laboratory, RIKEN Cluster for Pioneering Research, 2-1 Hirosawa, Wako, Saitama 351-0198, Japan
Tel +81 48 467 5809
Fax +81 48 467 9300
Email y-ito@riken.jp

submit your manuscript | www.dovepress.com
DovePress
http://doi.org/10.2147/IJN.S217416

electrically conductive polymer polypyrrole with some surface modifications.[19–21] The material stiffness is also considered to be important.[22] In addition to these physical parameters, topographical factors have been recently taken into consideration.[23–28]

In this study, we prepared a nanolayer of NGF-immobilized substrate that induced neurite outgrowth resulting in nerve regeneration to investigate biochemical and topographical effects. The photo-immobilization method using photoreactive gelatin (P-gel), which contains azido phenyl groups, was used for the immobilization as reported previously.[29–31] Micropatterns were prepared using photomasks, and topographical (thickness) regulation was achieved by the amount of cast P-gel. A rat adrenal pheochromocytoma cell line (PC12) was used as an in vitro model. Some cell lines are used as neuronal cell models.[32] The PC12 cell is one of them, and it has been widely used as a model for neural differentiation.[32,33] Although it is not originally a neuronal cell type, its neurite formation has been extensively investigated.[10,12,13,17,19–21,34–37] Because neurite outgrowth can be simultaneously correlated with diverse cues in developing neurons, we investigated cellular behaviors on the immobilized surface at various concentrations and used a micropatterned substrate that modulates neurite formation and outgrowth.

Materials and methods

Materials

PC12 cells were purchased from the Japanese Collection of Research Bioresources Cell Bank (Tokyo, Japan). Plastic plates (15 mm in diameter) were purchased from Thermo Fisher Scientific (Waltham, MA, USA). Rhβ-NGF was purchased from R&D Systems (Minneapolis, MN, USA). Gelatin from porcine skin (Type A) and a Rat β-NGF ELISA Kit were purchased from Sigma-Aldrich (St. Louis, MO, USA). A primary antibody (rabbit polyclonal against NGF) and secondary antibody (Alexa Fluor 488 goat anti-rabbit IgG) were purchased from Abcam (Cambridge, UK) and Thermo Fisher Scientific, respectively.

Preparation of photoreactive gelatin

P-gel was synthesized according to a previously reported method.[31] Briefly, gelatin powder (200 mg) was completely dissolved in Milli-Q water (100 mL). *N*-(4-Azidobenzoyloxy) succinimide prepared from 4-azidobenzoic acid (Tokyo Kasei Industry, Tokyo, Japan) dissolved in 1,4-dioxane (4 mL) was added to the gelatin solution. The mixture was stirred at room temperature for 2 days. The resulting solution was dialyzed against Milli-Q water twice. P-gel was recovered as a powder by a freeze-dry process. The content of azidophenyl groups in the gelatin was determined based on the absorbance of azidophenyl groups (λ: 270 nm) using a V-550 spectrophotometer (JASCO, Tokyo, Japan).

Surface immobilization of NGF

NGF was immobilized on the plastic plate as shown in Figure 1. The aqueous solution of P-gel was poured (20 μL per plate) onto the plate. After drying in air at room temperature, the plate was irradiated by a UV spot light lamp (Hamamatsu Photonics, Hamamatsu, Japan) at 10 cm from the light source (12 mW/cm^2) for 10 s, and then

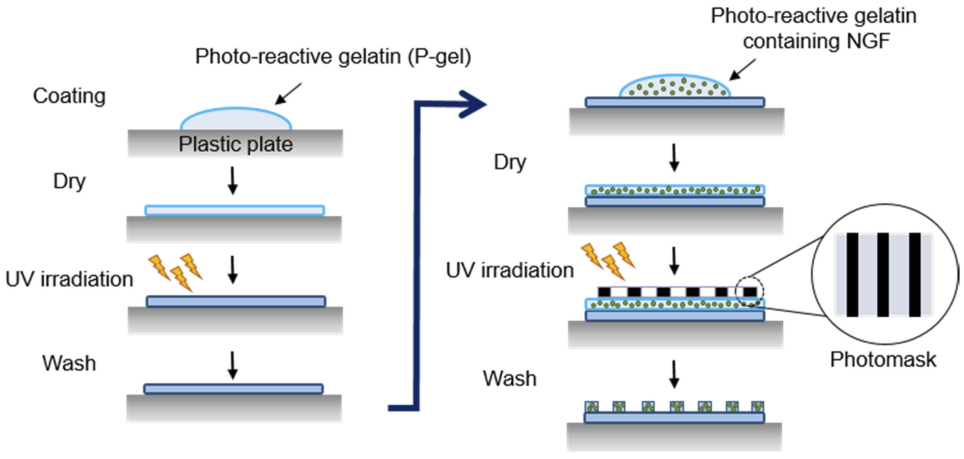

Figure 1 Schematic illustration of photo-immobilization. Steps in immobilization of NGF by photoreactive gelatin (P-gel) with photomask patterning. P-gel was immobilized on the plastic plate without the photomask in the first step of immobilization. In the second step, P-gel and NGF were immobilized on the P-gel-immobilized layer with the photomask.

washed with Milli-Q water. Subsequently, P-gel solutions containing NGF at various concentrations (0.35–3.5 pmol/per well plate) was poured onto the P-gel-immobilized plate. After drying in air while protected from light at room temperature, the plate was exposed to UV light under the same condition described above with or without a photomask (Toppan Printing, Tokyo, Japan). The plate was then washed with Milli-Q water repeatedly.

Determination of the amount of immobilized NGF

After the NGF-immobilized sample was repeatedly washed with Milli-Q water until no NGF was confirmed, the wash solutions were collected. The amount of NGF in the collected solutions was determined by the Rat β-NGF ELISA Kit, in accordance with the manufacturer's protocol. The amount of immobilized NGF was calculated by subtraction of the washed out NGF from the initial amount of NGF.

Staining of the NGF-immobilized surface

The NGF-immobilized substrate was blocked with 0.5% goat serum and incubated with the primary antibody for 1 h at room temperature. After three washes with Milli-Q water, the surface was incubated with the secondary antibody in the dark for 1 h at room temperature. The fluorescent signal was observed using a fluorescence microscope (IX71, Olympus, Tokyo, Japan).

Morphological characterization of materials

A reflective confocal laser microscope (RLCM, OLS4100, Olympus, Tokyo, Japan) was used to observe the morphology of gelatin-immobilized micropatterned surfaces. After the sample was placed on the stage of the RCLM, the multiple mirrors of the RCLM scanned the laser across the sample. The image was obtained across a fixed pinhole and detector, and the thickness of the formed layer was measured. All procedures of RCLM measurements were conducted in a clean room to avoid any contamination of the surface.

Cell culture

PC12 cells were cultured in Roswell Park Memorial Institute medium-1640 (RPMI-1640) (Sigma-Aldrich) supplemented with 10% fetal bovine serum (FBS, MP Biomedicals, Quebec, Canada) and 5% horse serum (HS, Life technologies, Carlsbad, CA). The cells were cultured in an incubator at 37 °C with 5% CO_2. At 70–80% confluence, the cells were harvested or sub-cultured with 0.25% trypsin and 1 mM ethylenediaminetetraacetic acid (EDTA). To investigate NGF effects, the culture medium was replaced with differentiation medium containing 1.0% FBS and 0.5% HS. After the cells were cultured for 2 days, they were then analyzed.

Scanning electron microscopy (SEM) analysis

After cell culture on the substrate, the samples were rinsed with PBS and fixed with 2.5% glutaraldehyde in 0.1 M sodium cacodylate (pH 7.4) overnight. The samples were then rinsed with 0.1 M sodium cacodylate and dehydrated sequentially via an aqueous replacement process by soaking in a series of 60%, 80%, and 100% ethanol solutions. Finally, the samples were transferred to 100% hexamethyldisilazane for 10 min and then dried overnight. The prepared samples were observed under a scanning electron microscope (Thermo Fisher Quattro SEM, Thermo Fisher Scientific).

Estimation of neurite formation

Neurite formation of the PC12 cell body was analyzed using ImageJ and Neuron J programs as reported previously.[38–40] The calculation images are shown in Figures S1 and S2. To determine neurite lengths, the neurites were segmented from the cell body and traced by automated tracing of the software. Then, the length was calculated by the "Analyze skeleton" plugin.[40] For each substrate, the neurite length was calculated using at least 30 neurites in five independent fields of each image from three different images.

To determine the frequency of neurite-forming cells, the cells were categorized into neurite-forming and non-forming neurites.[39,40] If at least one neurite length in a cell was longer than the cell size, which was calculated by the longest width of the cell, the cell was defined as a neurite-forming cell (Cell B). Otherwise, cells were defined as non-neurite-forming cells (Cell A). The frequency of neurite extension was estimated according to the above definition and the following equation.[39] The value was calculated using 30 cells (Cell A + Cell B) in five independent fields of each image from three different images for each substrate.

$$\text{Frequency of neurite-extended cells } (\%) = \frac{\text{Cell B}}{\text{Cell A} + \text{Cell B}} \times 100$$

To analyze neurites crossing the pattern step, formed neurites were randomly chosen for each substrate, and the ratio of crossing the step was calculated as shown in Figure S2. The value was calculated using 30 neurites in five

independent fields of each image from three different images for each substrate.

To analyze neurite-guided cells, the neurite angle between a neurite and patterned direction was determined based on previous reports.[41,42] Neurite-formed cells were randomly chosen and the longest neurite of the cells was analyzed. When the angle of the longest neurite with the cell body was lower than 15°, as shown in Figure S3, the neurite-formed cell was categorized as a neurite-aligned cell (Cell B). Otherwise, cells were defined as non-neurite-aligned cells (Cell A). The value was calculated using 30 cells (Cell A + Cell B) in five independent fields of each image from three different images for each substrate.

$$\text{Ratio of neurite-guided cells } (\%) = \frac{\text{Cell B}}{\text{Cell A} + \text{Cell B}} \times 100$$

Statistical analysis

Data were presented as the mean ± standard deviation (S.D.). Statistical comparisons were performed by the Student's *t*-test and one-way ANOVA followed by the Tukey post-hoc test. $P<0.05$ was considered as statistically significant.

Results and discussion

Immobilization of NGF

P-gel has specific UV absorbance at 270 nm ascribed to the azidophenyl group (Figure S4). Upon UV irradiation, the azidophenyl groups in P-gel decompose to form nitrene as a reactive radical to crosslink the NGF, P-gel, and substrate. After these crosslinking reactions, NGF was covalently immobilized to P-gel, covalently immobilized to the substrate surface through P-gel, or entrapped in the cross-linked P-gel. This immobilization was confirmed by pattern staining of immobilized NGF (Figure 2). The images show green fluorescence from the Alexa 488-conjugated antibody only on the NGF-immobilized area.

Figure S6A–D show that the efficiency of NGF immobilization in the P-gel layer increased with increasing the amount of P-gel and NGF. As summarized in Figure 3, 100% immobilization of various amounts of NGF (1, 5, 20, and 50 ng) was achieved by 0.1% and 0.5% P-gel. Based on these conditions for NGF immobilization, the samples were prepared with the minimal required amount of P-gel (0.1%) to reduce the effect of P-gel in further in vitro experiments.

Preparation of the micropatterned surface

The difference between immobilized and non-immobilized regions, where two layers were achieved by the photomask, was observed by phase contrast microscopy (Figure S5). The micropattern treatment using a small amount of gelatin such as 0.01% was insufficient to be observed by phase contrast microscopy because the layer was too thin. However, the micropatterns using 0.1% and 1.0% gelatin were sufficient for observation.

The RCLM technique was employed to quantitatively evaluate the immobilized surface (Figure 4). The thickness of the layers prepared using different amounts of P-gel was determined. The theoretical thickness was calculated from the amount of cast gelatin on the substrate. Using the density of gelatin (1.27 g/cm^3),[43] the volume was calculated. Finally, the volume was divided by the surface area (15 mm diameter of the plastic disc) to calculate the

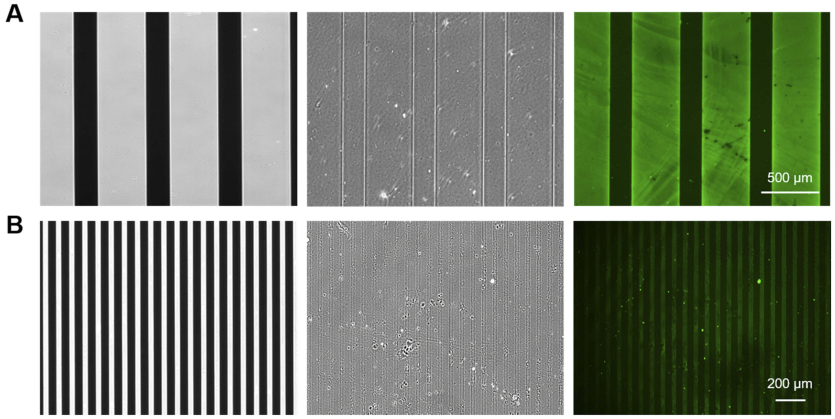

Figure 2 Visualization of the NGF-micropatterned surface. Phase contrast images of the photomask (left) and micropatterned surface formed by photoreactive gelatin with the photomask (middle). Immunofluorescence images of the immobilized NGF (right). The wide (**A**)- and narrow (**B**)-patterned substrates were prepared by photomasks with different linear patterns.

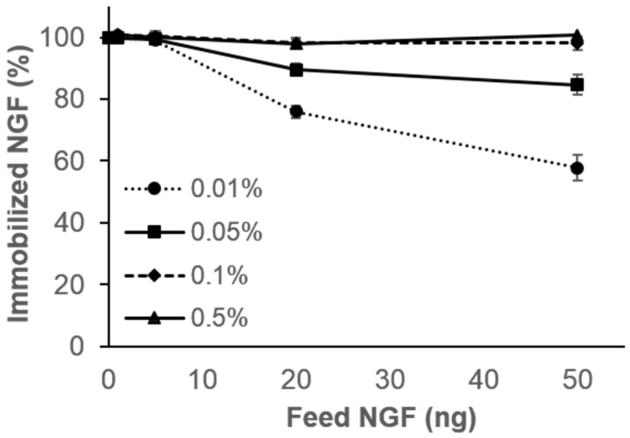

Figure 3 Measurement of immobilized NGF on the substrate by ELISA. Percentages of immobilized NGF (1, 5, 20, and 50 ng) in the gelatin solution using various concentrations of P-gel (0.01%, 0.05%, 0.1%, and 0.5%). Data are presented as the mean ± SD, n=3.

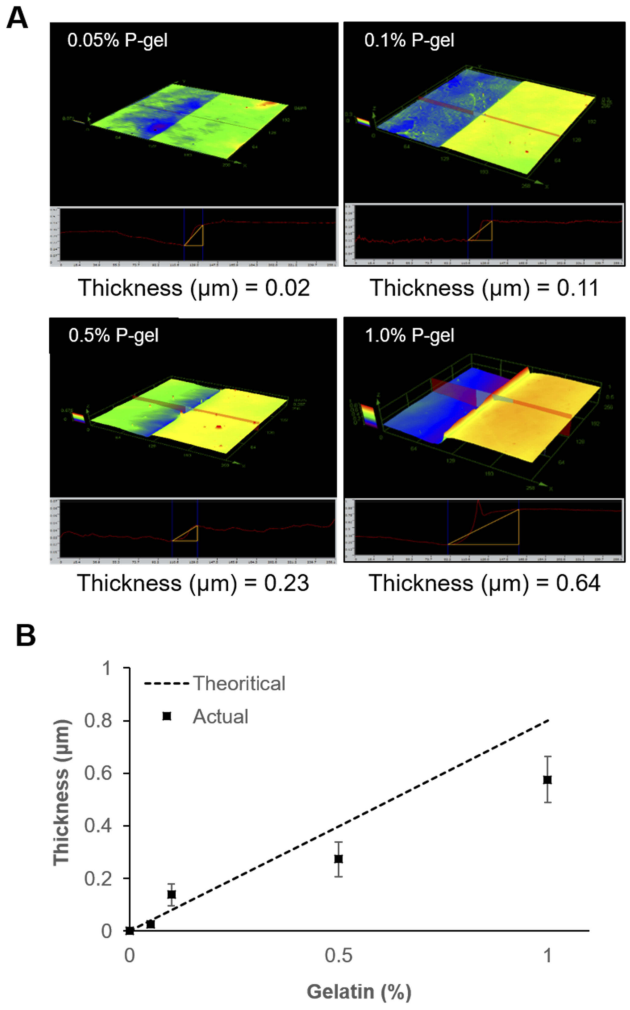

Figure 4 Characteristics of the immobilized surface by P-gel. (**A**) 3D measurement using a reflective confocal laser microscope (RCLM) to observe the morphological structure of the immobilized surface at different concentrations of P-gel. (**B**) Comparison of the thickness on immobilized substrates. Data are presented as the mean ± SD, n=3.

height. The thickness on the immobilized layers was very close to the theoretical thickness. This result indicates that the surface thickness can be easily controlled by changing the concentration of P-gel. Therefore, we could employ in vitro cell cultures to understand neuronal behaviors on the different topographical surfaces.

Cellular behavior on surfaces with micropattern-immobilized NGF

To investigate the effect of NGF immobilization on cellular behavior, PC12 cells were cultured on the micropattern-immobilized NGF as shown in Figure 5. The micropatterning enabled us to observe the effect of immobilized NGF at a glance. Although the cells were randomly distributed on both non-immobilized and NGF-immobilized regions when they were seeded, the cell density was higher on the NGF-immobilized regions during culture. The increase in cell number on the NGF-immobilized regions was considered to be due to the migration of cells and their gradual trapping by immobilized NGF. On the immobilized regions, significant neurite outgrowth was also observed. The micropattern-immobilized NGF substrate simultaneously showed both trapping of cells and neurite outgrowth.

Quantitative comparison of soluble and immobilized NGF

Neurite extension and formation were characterized under the different states of NGF (soluble and immobilized) as shown in Figure 6. By increasing the amount of NGF, both soluble and immobilized NGF increased the neurite length and the frequency of extended neurites. This effect was saturated at >1 pmol/well plate. The immobilized NGF had almost the same effect on neurite formation of PC12 cells as soluble NGF. Yu et al[9] described almost the same effect on neuron survival (70%) after 3 days of culture using 30 ng/cm^2 chitosan-immobilized NGF and 50 ng/mL soluble NGF. Lee et al[20] demonstrated that almost the same effect on PC12 neurite formation (30%, 14 μm length) was achieved by both immobilized NGF and 50 ng/mL soluble NGF. The immobilized NGF at 30 ng/cm^2 reported by Yu et al[9] corresponds to 1.5 pmol/well plate in the present study, and the soluble NGF at 50 ng/mL reported by Lee et al[20] corresponds to 1.7 pmol/well plate in the present study. Therefore, the present results indicate that the same effect was achieved by the same amounts of NGF as reported previously.

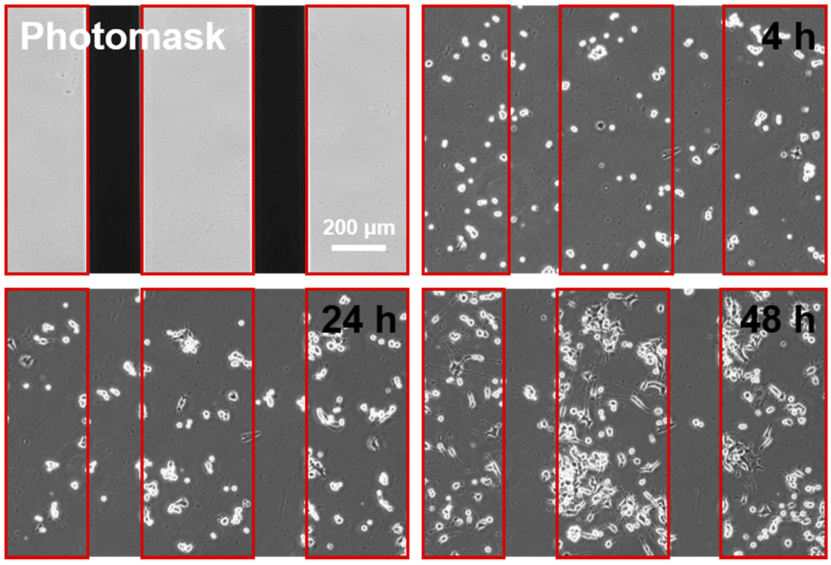

Figure 5 Cellular behavior on the micropattern-immobilized NGF substrate. Based on a linear pattern photomask, the non-immobilized region (shaded area of the photomask) and NGF-immobilized region (open area of the photomask; Red line) were 200 and 400 μm, respectively.

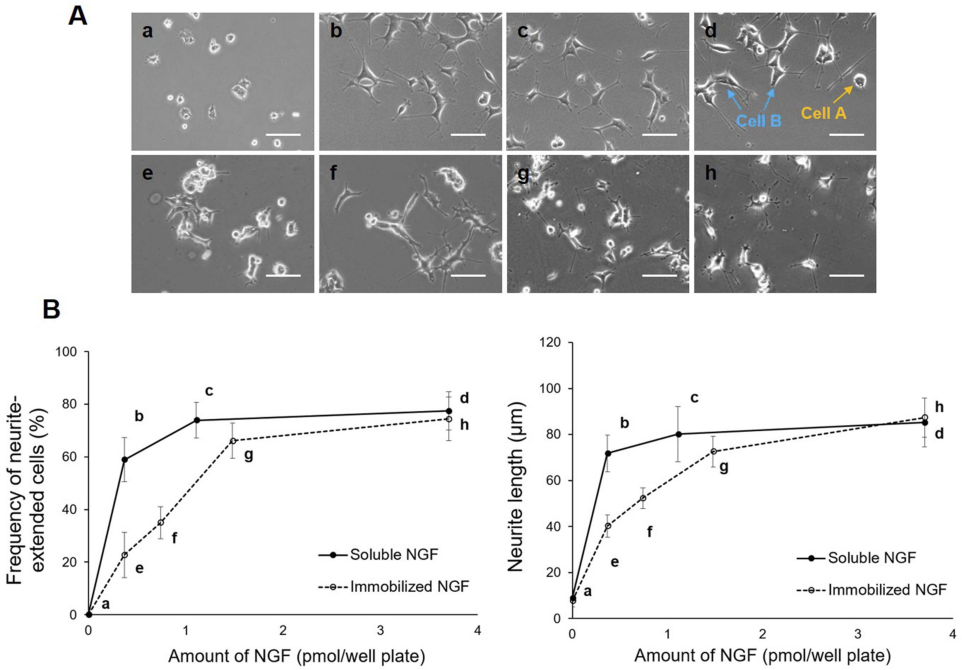

Figure 6 Characterization of neuronal behavior under soluble and immobilized NGF conditions. (**A**) Representative images of cellular morphology at various concentrations of soluble and immobilized NGF. No NGF; Negative control (**A**), soluble NGF; 0.35, 1.0, and 3.5 pmol/well plate (a–d), immobilized NGF; 0.35, 0.75, 1.5, and 3.5 pmol/well plate (e–h). Scale bar: 100 μm. (**B**) Frequency of neurite-extended cells and neurite length with soluble and immobilized NGF. Data are presented as the mean ± SD, n=3.

Immobilized growth factors, such as insulin, epidermal growth factor (EGF), and fibroblast growth factor, enhance cell growth more than soluble growth factors by inhibiting the downregulation of signal transduction caused by cellular internalization of growth factors.[44–46] It has also been reported that immobilized EGF promotes neurite formation of PC12 cells, although soluble EGF enhances the growth of PC12 cells.[47]

In the case of NGF immobilization, neither promotion of neurite formation nor switching of gene expression occurred. The signal transduction mechanism of growth is different

from that of differentiation in PC12 cells.[48] It is also well known that the differentiation depends on sustained signaling.[49] However, the nerve growth cone exhibits adaptation through desensitization and resensitization to wide ranges of concentrations of guidance factors[50] and the downregulation depends on the endocytosis of receptors.[51] Considering these studies, cone guidance is up/downregulated but neurite formation requires sustained and monotonous signaling. Therefore, it was considered that no downregulation process that generally occurred in the growth process occurred in the differentiation process. As a result, a specific difference between soluble and immobilized NGF was found in neurite formation.

Thermal stability and reusability of immobilized NGF

To investigate the thermal stability of immobilized NGF, samples were incubated at 37, 42, and 60 °C for various durations (Figure 7). Although significant loss of soluble NGF activity was observed, the immobilized NGF showed a lesser decrease of activity at any temperature. Therefore, the immobilization maintained the biological activity of NGF through reduction of the conformational flexibility of NGF by fixation as observed in enzymes.[52,53]

To confirm the stability of immobilized NGF, it was repeatedly used after cell culture as shown in Figure 8. The results showed no significant decrease in the biological activity

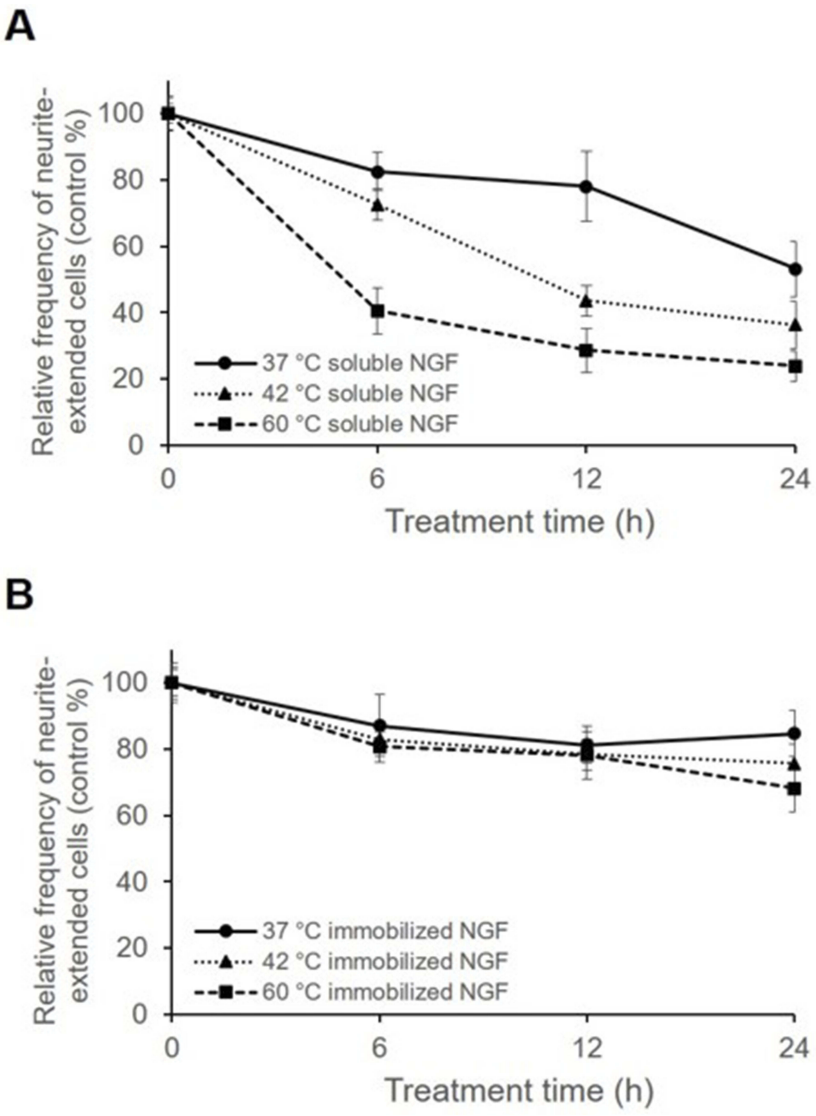

Figure 7 Frequency of neurite-extended cells cultured with soluble NGF and immobilized NGF pretreated at 37, 42, and 60 °C for 6, 12, and 24 h. Cells cultured with soluble and immobilized NGF without pretreatment were used as controls, and cells at 0 h were considered as 100%. Cells were cultured with either (**A**) pretreated soluble NGF in growth medium or (**B**) pretreated immobilized NGF. Data are presented as the mean ± SD, n=3.

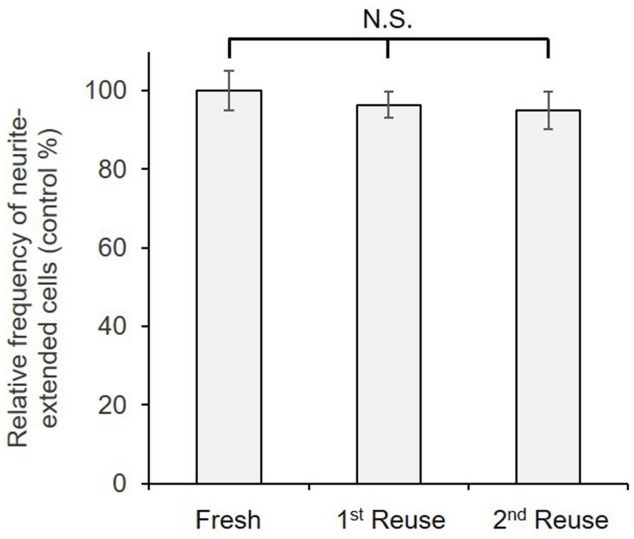

Figure 8 Frequency of neurite-extended cells cultured on immobilized NGF that was reused twice. Cells cultured on a freshly prepared surface with immobilized NGF were used as controls and considered as 100%. Data are presented as the mean ± SD, n=3. N.S., no significant difference.

of the reused plates with immobilized NGF in comparison with that of the fresh plates. Figure 8 shows at least two reuses without losing the biological activity that induced neurite outgrowth. Taken into consideration with other previous reports,[31,53] we concluded that the reusability of biomolecules, such as growth factors, enzymes, and antibodies, may be facilitated by immobilization.

Neurite guidance on the micropatterned surface

The contact guidance of formed neurites was investigated on the different thicknesses of micropatterned layers in the presence of 100 ng/mL soluble NGF as shown in Figure 9. In the case of a low height (26 nm) of the step, the neurites had sporadically formed and outgrew regardless of the patterned surface. However, in the case of a high height (>130 nm), the neurites had extended and aligned on the borderline of the two layers. Considering the largest diameter of a neurite was 30–40 nm, a 100 nm layer thickness was sufficient for contact guidance of neurites.

Previously Chua et al[41] and Béduer et al[42] reported the neurite guidance by microfabricated polydimethylsiloxane (PDMS). According to Chua et al, the height ranged from 350 to 4,000 nm, and the neurite alignment of

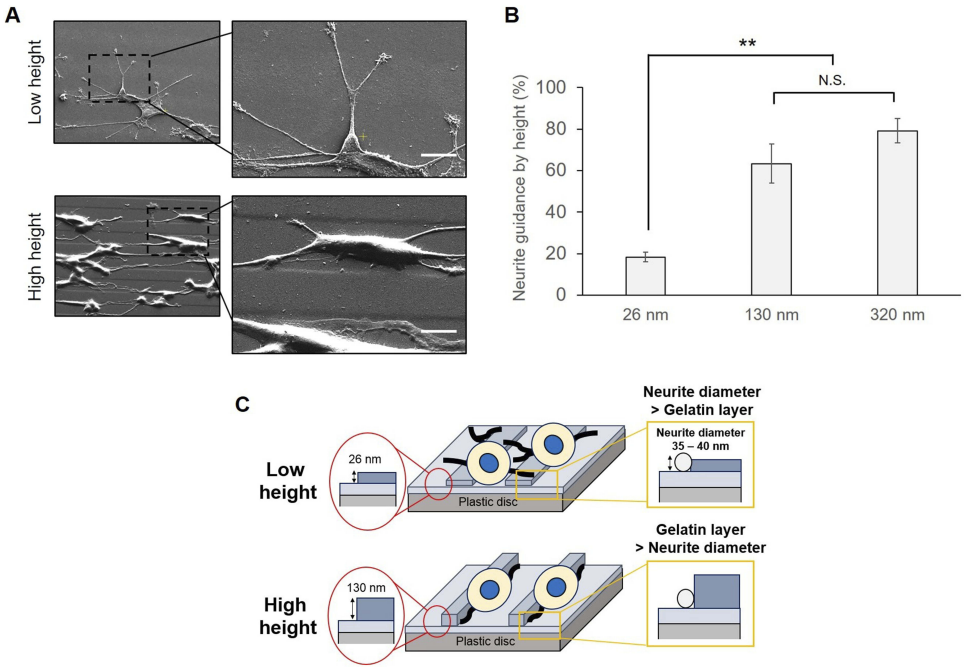

Figure 9 Control of neurite direction by the immobilized height. (**A**) Observation of the cellular response to different heights by SEM analysis. The micropatterned surface was prepared by a narrow linear pattern using a photomask (10 μm: 15 μm). Scale bar: 10 μm. NGF at 3.5 pmol was added in each well. (**B**) Comparison of neurite guidance by height. Neurite guidance was estimated on gelatin-immobilized substrates with different heights and soluble NGF. The height between the first and second gelatin layers was adjusted by different concentrations of gelatin. NGF at 3.5 pmol was added in each well. (**C**) Schematic illustration for neurite formation by the relationship between the neurite diameter and immobilized height. Data are presented as the mean ± SD, n=3. N.S., no significant difference, $^{**}P<0.01$; significant difference.

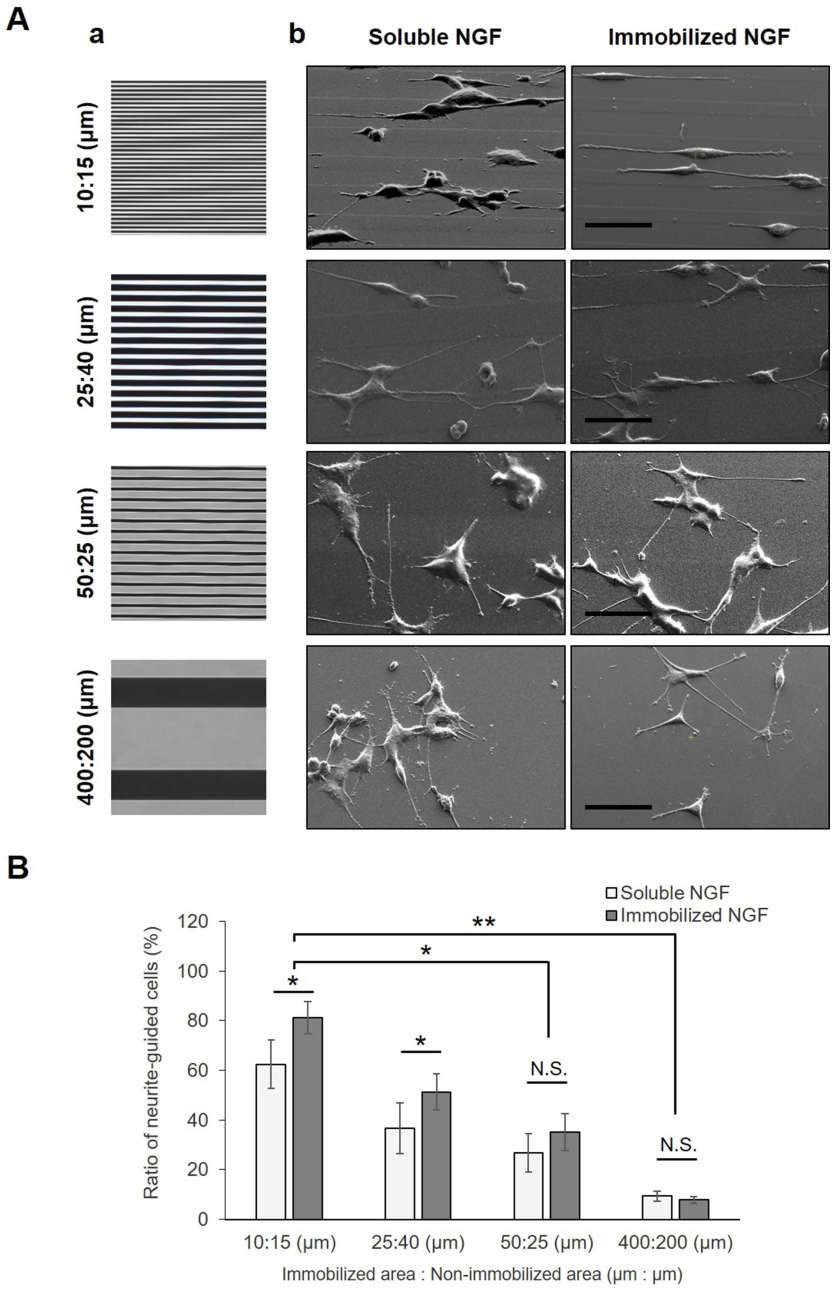

Figure 10 Guidance of the neurite direction by different micropatterned surfaces. (**A**) Photomasks with different linear patterns (a) and SEM images (b) of outgrowing neurites of PC12 cells on micropatterned substrates. Prior to cell culture, all substrates were immobilized by gelatin through a photomask with various linear ratios between UV-transparent (NGF-immobilized area) and non-transparent (non-immobilized area) regions. In the case of soluble NGF, the NGF was added to the growth medium to assist in neurite outgrowth upon cell cultivation. Scale bar: 50 μm. (**B**) Estimation of neurite guidance. To compare neural interpreting of different micropatterned substrates, the ratio of neurite-guided cells was estimated. Data are presented as the mean ± SD, n=3. N.S., no significant difference, **P*<0.05; significant difference, ***P*<0.01; significant difference.

hippocampal murine neural progenitor cells monotonously increased with the increase in height. Considering that the present material was based on gelatin, the greater adhesiveness than PDMS for neurites may reduce the threshold height that a cell can recognize.

Because contact guidance of neurites was achieved by a 100 nm height of the step wall, neurite alignment from the cell was investigated on different widths of micropatterns as shown in Figure 10. The neurites of PC12 cells cultured on the most narrow micropatterned surfaces (10 μm: 15 μm) showed that many cells formed aligned neurites according to the patterned steps. Most cells on the patterns extended two or more neurites bidirectionally. When the micropattern width was enlarged, the neurite

orientations became more random. This result indicates that the neurite alignment of cells can be finely modulated when the number of gelatin-based steps increases.

Ferrari et al[54] performed nanotopographic control of PC12 cells on nanoprinted cyclic olefin copolymer films and found that a 500 nm width was the most effective for the formation of a bipolar shape, and that on a width larger than 1,500 nm, cells had the tendency to form a multipolar shape. However, Béduer et al[42] reported that a 60 μm groove width contributed more to alignment than an unpattern surface. The present study showed that neurites can be modulated by a sufficient height for neurite guidance and a sufficient narrow groove.

Figure 10 also indicates that NGF immobilization increased the alignment of neurites. Considering that chick dorsal-root axons turn toward high concentrations of NGF[11] as well as NGF concentration-dependent neurite formation,[12,13] the enhanced alignment was due to the direct interaction between neurites and immobilized NGF.

Conclusion

NGF-immobilized nanolayers were prepared by photocrosslinking for neurite formation. The immobilized NGF induced neurite outgrowth similarly to soluble NGF, although the soluble NGF showed higher activity at a low concentration compared with immobilized NGF. The micropatterned layers showed guided neurite formation on certain micropatterned surfaces. Furthermore, the micropattern immobilization of NGF simultaneously showed biochemical and topographical effects on neurite formation.

Acknowledgment

This work was financially supported by KAKENNHI from JSPS (15H01810). S.M.K. was financially supported by the Junior Research Associate (JRA) program from RIKEN. We thank Dr. Hiroyuki Kamiguchi at the RIKEN Center for Brain Science for useful discussions. We also thank Mitchell Arico from Edanz Group for editing a draft of this manuscript.

Disclosure

The authors report no conflicts of interest in this work.

References

1. Schmidt CE, Leach JB. Neural tissue engineering: strategies for repair and regeneration. *Annu Rev Biomed Eng*. 2003;5:293–347. doi:10.1146/annurev.bioeng.5.011303.120731
2. Roach R, Parker T, Gadegaard N, Alexandera MR. Surface strategies for control of neuronal cell adhesion: a review. *Surf Sci Rep*. 2010;65(6):145–173. doi:10.1016/j.surfrep.2010.07.001
3. Nectow AR, Marra KG, Kaplan DL. Biomaterials for the development of peripheral nerve guidance conduits. *Tissue Eng Part B Rev*. 2012;18(1):40–50. doi:10.1089/ten.teb.2011.0240
4. Pinho AC, Fonseca AC, Serra AC, Santos JD, Coelho JF. Peripheral nerve regeneration: current status and new strategies using polymeric materials. *Adv Healthc Mater*. 2016;5(21):2732–2744. doi:10.1002/adhm.201600236
5. Simitzi C, Ranella A, Stratakis E. Controlling the morphology and outgrowth of nerve and neuroglial cells: the effect of surface topography. *Acta Biomater*. 2017;51:21–52. doi:10.1016/j.actbio.2017.01.023
6. Simitzi C, Karali K, Ranella A, Stratakis E. Controlling the outgrowth and functions of neural stem cells: the effect of surface topography. *Chemphyschem*. 2018;19(10):1143–1163. doi:10.1002/cphc.201701175
7. Ito Y. Regulation of cellular gene expression by artifcial materials immobilized with biosignal molecules. *Jpn J Artif Organs*. 1998;27(2):541–544. doi:10.11392/jsao1972.27.541
8. Kapur TA, Shoichet MS. Chemically-bound nerve growth factor for neural tissue engineering applications. *J Biomater Sci Polym Ed*. 2003;14(4):383–394. doi:10.1163/156856203321478883
9. Yu LM, Wosnick JH, Shoichet MS. Miniaturized system of neurotrophin patterning for guided regeneration. *J Neurosci Methods*. 2008;171(2):253–263. doi:10.1016/j.jneumeth.2008.03.023
10. Bhang SH, Lee TJ, Yang HS, La WG, Han AM, Kwon YH, Kim BS. Enhanced nerve growth factor efficiency in neural cell culture by immobilization on the culture substrate. *Biochem Biophys Res Commun*. 2009;382(2):315–320. doi:10.1016/j.bbrc.2009.03.016
11. Gundersen RW, Barrett JN. Neuronal chemotaxis: chick dorsal-root axons turn toward high concentrations of nerve growth factor. *Science*. 1979;206(4422):1079–1080. doi:10.1126/science.493992
12. Cao X, Shoichet MS. Defining the concentration gradient of nerve growth factor for guided neurite outgrowth. *Neuroscience*. 2001;103(3):831–840. doi:10.1016/S0306-4522(01)00029-X
13. Kapur TA, Shoichet MS. Immobilized concentration gradients of nerve growth factor guide neurite outgrowth. *J Biomed Mater Res A*. 2004;68(2):235–243. doi:10.1002/jbm.a.10168
14. Dontchev VD, Letourneau PC. Nerve growth factor and semaphorin 3A signaling pathways interact in regulating sensory neuronal growth cone motility. *J Neurosci*. 2002;22(15):6659–6669. doi:10.1523/JNEUROSCI.22-15-06659.2002
15. Joddar B, Guy AT, Kamiguchi H, Ito Y. Spatial gradients of chemotropic factors from immobilized patterns to guide axonal growth and regeneration. *Biomaterials*. 2013;34(37):9593–9601. doi:10.1016/j.biomaterials.2013.08.019
16. McCormick AM, Wijekoon A, Leipzig ND. Specific immobilization of biotinylated fusion proteins NGF and Sema3A utilizing a photocross-linkable diazirine compound for controlling neurite extension. *Bioconjug Chem*. 2013;24(9):1515–1526. doi:10.1021/bc400058n
17. Achyuta AK, Cieri R, Unger K, Murphy SK. Synergistic effect of immobilized laminin and nerve growth factor on PC12 neurite outgrowth. *Biotechnol Prog*. 2009;25(1):227–234. doi:10.1002/btpr.58
18. Anderson M, Shelke NB, Manoukian OS, Yu X, McCullough LD, Kumbar SG. Peripheral nerve regeneration strategies: electrically stimulating polymer based nerve growth conduits. *Crit Rev Biomed Eng*. 2015;43(2–3):131–159. doi:10.1615/CritRevBiomedEng.2015014015
19. Gomez N, Schmidt CE. Nerve growth factor-immobilized polypyrrole: bioactive electrically conducting polymer for enhanced neurite extension. *J Biomed Mater Res A*. 2007;81(1):135–149. doi:10.1002/jbm.a.31047
20. Lee JY, Bashur CA, Milroy CA, Forciniti L, Goldstein AS, Schmidt CE. Nerve growth factor-immobilized electrically conducting fibrous scaffolds for potential use in neural engineering applications. *IEEE Trans Nanobioscience*. 2012;11(1):15–21. doi:10.1109/TNB.2011.2159621

21. Zeng J, Huang Z, Yin G, Qin J, Chen X, Gu J. Fabrication of conductive NGF-conjugated polypyrrole-poly(l-lactic acid) fibers and their effect on neurite outgrowth. *Colloids Surf B Biointerfaces*. 2013;110:450–457. doi:10.1016/j.colsurfb.2013.05.012
22. Leipzig ND, Shoichet MS. The effect of substrate stiffness on adult neural stem cell behavior. *Biomaterials*. 2009;30(36):6867–6878. doi:10.1016/j.biomaterials.2009.09.002
23. Jang KJ, Kim MS, Feltrin D, Jeon NL, Suh KY, Pertz O. Two distinct filopodia populations at the growth cone allow to sense nanotopographical extracellular matrix cues to guide neurite outgrowth. *PLoS One*. 2010;5(12):e15966. doi:10.1371/journal.pone.0015966
24. Houchin-Ray T, Huang A, West ER, Zelivyanskaya M, Shea LD. Spatially patterned gene expression for guided neurite extension. *J Neurosci Res*. 2009;87(4):844–856. doi:10.1002/jnr.21908
25. Marquardt LM, Sakiyama-Elbert SE. Engineering peripheral nerve repair. *Curr Opin Biotechnol*. 2013;24(5):887–892. doi:10.1016/j.copbio.2013.05.006
26. Honegger T, Thielen MI, Feizi S, Sanjana NE, Voldman J. Microfluidic neurite guidance to study structure-function relationships in topologically-complex population-based neural networks. *Sci Rep*. 2016;6:28384. doi:10.1038/srep28384
27. Sharma AD, Zbarska S, Petersen EM, Marti ME, Mallapragada SK, Sakaguchi DS. Oriented growth and transdifferentiation of mesenchymal stem cells towards a Schwann cell fate on micropatterned substrates. *J Biosci Bioeng*. 2016;121(3):325–335. doi:10.1016/j.jbiosc.2015.07.006
28. Chan LY, Birch WR, Yim EK, Choo AB. Temporal application of topography to increase the rate of neural differentiation from human pluripotent stem cells. *Biomaterials*. 2013;34(2):382–392. doi:10.1016/j.biomaterials.2012.09.033
29. Ito Y, Hasuda H, Yamauchi T, Komatsu N, Ikebuchi K. Immobilization of erythropoietin to culture erythropoietin-dependent human leukemia cell line. *Biomaterials*. 2004;25(12):2293–2298. doi:10.1016/j.biomaterials.2003.09.002
30. Kitajima T, Obuse S, Adachi T, Tomita M, Ito Y. Recombinant human gelatin substitute with photoreactive properties for cell culture and tissue engineering. *Biotechnol Bioeng*. 2011;108(10):2468–2476. doi:10.1002/bit.23192
31. Mao H, Kim SM, Ueki M, Ito Y. Serum-free culturing of human mesenchymal stem cells with immobilized growth factors. *J Mater Chem B*. 2017;5:928–934. doi:10.1039/C6TB02867E
32. Gordon J, Amini S, White MK. General overview of neuronal cell culture. *Methods Mol Biol*. 2013;1078:1–8. doi:10.1007/978-1-62703-640-5_1
33. Westerink RH, Ewing AG. The PC12 cell as model for neurosecretion. *Acta Physiol (Oxf)*. 2008;192(2):273–285. doi:10.1111/j.1748-1716.2007.01805.x
34. Katebi S, Esmaeili A, Ghaedi K, Zarrabi A. Superparamagnetic iron oxide nanoparticles combined with NGF and quercetin promote neuronal branching morphogenesis of PC12 cells. *Int J Nanomedicine*. 2019;14:2157–2169. doi:10.2147/IJN.S191878
35. Haq F, Anandan V, Keith C, Zhang G. Neurite development in PC12 cells cultured on nanopillars and nanopores with sizes comparable with filopodia. *Int J Nanomedicine*. 2007;2(1):107–115. doi:10.2147/nano.2007.2.1.107
36. Alhosseini SN, Moztarzadeh F, Mozafari M, Asgari S, Dodel M, Samadikuchaksaraei A, Kargozar S, Jalali N. Synthesis and characterization of electrospun polyvinyl alcohol nanofibrous scaffolds modified by blending with chitosan for neural tissue engineering. *Int J Nanomedicine*. 2012;7:25–34. doi:10.2147/IJN.S25376
37. Wei GJ, Yao M, Wang YS, Zhou CW, Wan DY, Lei PZ, Wen J, Lei HW, Dong DM. Promotion of peripheral nerve regeneration of a peptide compound hydrogel scaffold. *Int J Nanomedicine*. 2013;8:3217–3225. doi:10.2147/IJN.S43681
38. Pool M, Thiemann J, Bar-Or A, Fournier AE. Neurite tracer: a novel imagej plugin for automated quantification of neurite outgrowth. *J Neurosci Methods*. 2008;168(1):134–139. doi:10.1016/j.jneumeth.2007.08.029
39. Yu W, Lee HK, Hariharan S, Bu W, Ahmed S. Quantitative neurite outgrowth measurement based on image segmentation with topological dependence. *Cytom A*. 2009;75(4):289–297. doi:10.1002/cyto.a.20664
40. Haas AJ, Prigent S, Dutertre S, Le Dréan Y, Le Page Y. Neurite analyzer: an original Fiji plugin for quantification of neuritogenesis in two-dimensional images. *J Neurosci Methods*. 2016;271:86–91. doi:10.1016/j.jneumeth.2016.07.011
41. Chua JS, Chng CP, Moe AA, Tann JY, Goh EL, Chiam KH, Yim EK. Extending neurites sense the depth of the underlying topography during neuronal differentiation and contact guidance. *Biomaterials*. 2014;35(27):7750–7761. doi:10.1016/j.biomaterials.2014.06.008
42. Béduer A, Vieu C, Arnauduc F, Sol JC, Loubinoux I, Vaysse L. Engineering of adult human neural stem cells differentiation through surface micropatterning. *Biomaterials*. 2012;33(2):504–514. doi:10.1016/j.biomaterials.2011.09.073
43. Lide DR. CRC handbook of chemistry and physics, 84th ed. Boca Raton: CRC Press; 2003-2004.
44. Ito Y. Surface micropatterning to regulate cell functions. *Biomaterials*. 1999;20(23–24):2333–2342. doi:10.1016/S0142-9612(99)00162-3
45. Ito Y. Covalently immobilized biosignal molecule materials for tissue engineering. *Soft Matter*. 2008;4:46–56. doi:10.1039/B708359A
46. Ito Y. Growth factor engineering for biomaterials. *ACS Biomater Sci Eng*. In press 2019. doi:10.1021/acsbiomaterials.8b01649
47. Ito Y, Chen G, Imanishi Y, Morooka T, Nishida E, Okabayashi Y, Kasuga M. Differential control of cellular gene expression by diffusible and non-diffusible EGF. *J Biochem*. 2001;129(5):733–737. doi:10.1093/oxfordjournals.jbchem.a002913
48. Vaudry D, Stork PJ, Lazarovici P, Eiden LE. Signaling pathways for PC12 cell differentiation: making the right connections. *Science*. 2002;296(5573):1648–1649. doi:10.1126/science.1071552
49. Sun P, Watanabe H, Takano K, Yokoyama T, Fujisawa J, Endo T. Sustained activation of M-Ras induced by nerve growth factor is essential for neuronal differentiation of PC12 cells. *Genes Cells*. 2006;11(9):1097–1113. doi:10.1111/j.1365-2443.2006.01002.x
50. Ming GL, Wong ST, Henley J, Yuan XB, Song HJ, Spitzer NC, Poo MM. Adaptation in the chemotactic guidance of nerve growth cones. *Nature*. 2002;417(6887):411–418. doi:10.1038/nature745
51. Piper M, Salih S, Weinl C, Holt CE, Harris WA. Endocytosis-dependent desensitization and protein synthesis-dependent resensitization in retinal growth cone adaptation. *Nat Neurosci*. 2005;8(2):179–186. doi:10.1038/nn1380
52. Mateo C, Grazu V, Palomo JM, Lopez-Gallego F, Fernandez-Lafuente R, Guisan JM. Immobilization of enzymes on heterofunctional epoxy supports. *Nat Protoc*. 2007;2(5):1022–1033. doi:10.1038/nprot.2007.133
53. DiCosimo R, McAuliffe J, Poulose AJ, Bohlmann G. Industrial use of immobilized enzymes. *Chem Soc Rev*. 2013;42(15):6437–6474. doi:10.1039/c3cs35506c
54. Ferrari A, Cecchini M, Dhawan A, Micera S, Tonazzini I, Stabile R, Pisignano D, Beltram F. Nanotopographic control of neuronal polarity. *Nano Lett*. 2011;11(2):505–511. doi:10.1021/nl103349s